Structures and magnetic properties of Co(II)Cu(II) and Ni(II)Cu(II) compounds incorporating the obp = oxamidobis(*N,N'*-propionato) ligand

Anne Gulbrandsen and Jorunn Sletten
Department of Chemistry, University of Bergen, 5007 Bergen (Norway)

Keitaro Nakatani, Yu Pei and Olivier Kahn*
Laboratoire de Chimie Inorganique, URA CNRS No. 420, Université de Paris Sud, 91405 Orsay (France)

(Received February 8, 1993)

Abstract

Two novel bimetallic compounds have been prepared from the copper(II) precursor $[Cu(obp)]^{2-}$, namely $CoCu(obp)(H_2O)_3 \cdot H_2O$ (**1**) and $NiCu(obp)(H_2O)_5 \cdot 3.5H_2O$ (**2**), obp standing for oxamidobis(*N,N'*-propionato). The crystal structures of **1** and **2** have been solved. Both compounds crystallize in the triclinic system, space group $P\bar{1}$. The lattice parameters for **1** are $a = 8.642(1)$, $b = 9.197(1)$, $c = 10.645(2)$ Å, $\alpha = 67.14(1)$, $\beta = 62.28(1)$, $\gamma = 73.95(1)°$, $Z = 2$. Those of **2** are $a = 11.444(1)$, $b = 12.295(1)$, $c = 15.100(2)$ Å, $\alpha = 68.89(1)$, $\beta = 72.94(1)$, $\gamma = 76.26(1)°$, $Z = 4$ NiCu units. The structure of **1** consists of bimetallic chains in which the Co(II) and Cu(II) ions are alternately bridged by oxamido and carboxylato groups. In contrast, the structure of **2** consists of isolated oxamido-bridged Ni(II)Cu(II) units. The magnetic properties of both compounds have been investigated and quantitatively interpreted. In spite of its chain structure **1** does not show the one-dimensional ferrimagnetic behavior. It has been assumed that the interaction through the carboxylato bridged was very small. The magnetic data have been fitted with a model taking explicitly into account the orbital degeneracy of the Co(II) ion in a weak octahedral field. The magnetic behavior of **2** is in line with its structure with a strong intramolecular antiferromagnetic interaction between the spin carriers. Finally, the J_{MnCu}, J_{CoCu} and J_{NiCu} interaction parameters through the oxamido bridge in related compounds have been compared.

Introduction

Some years ago we described the first alternating bimetallic chain compound [1], of formula $MnCu(obp)(H_2O)_3 \cdot H_2O$, where obp stands for oxamidobis(*N,N'*-propionato). This compound was obtained by reaction of the copper(II) precursor $[Cu(obp)]^{2-}$, shown below

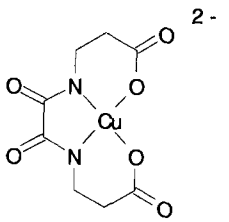

with the manganese(II) ion. The structure consists of chains with alternation of both the spin carriers, Mn(II) and Cu(II), and the bridges linking these spin carriers, oxamido and carboxylato. The magnetic properties of $MnCu(obp)(H_2O)_3 \cdot H_2O$ are characteristic of one-dimensional ferrimagnetism. Subsequently, we reported on other Mn(II)Cu(II) alternating bimetallic chain compounds, obtained from copper(II) precursors of the form

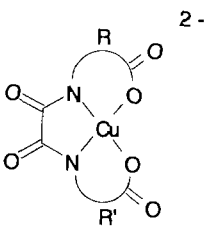

where R and R' may be identical or not, able to bond Mn(II) ions through both the oxamido group and one of the two carboxylato groups [2–7].

Since then, we have pursued our exploration of the chemistry of $[Cu(obp)]^{2-}$. Here, we report on the structures and magnetic properties of two novel com-

*Author to whom correspondence should be addressed.

0020-1693/93/$6.00

pounds, namely $CoCu(obp)(H_2O)_3 \cdot H_2O$ (**1**) and $NiCu(obp)(H_2O)_5 \cdot 3.5H_2O$ (**2**).

Experimental

Syntheses

The sodium salt of the copper(II) precursor, $Na_2[Cu(obp)] \cdot 3.5H_2O$, was prepared as already described [1]. Single crystals of $CoCu(obp)(H_2O)_3 \cdot H_2O$ (**1**) were obtained by slow evaporation at 50 °C of a solution containing 2 mmol of cobalt(II) perchlorate and 2 mmol of $Na_2[Cu(obp)] \cdot 3.5H_2O$ dissolved in 40 ml of water. Single crystals of $NiCu(obp)(H_2O)_5 \cdot 3.5H_2O$ (**2**) were obtained by slow evaporation at room temperature of a solution containing 2 mmol of nickel(II) perchlorate and 2 mmol of $Na_2[Cu(obp)] \cdot 3.5H_2O$ dissolved in 40 ml of a 4/1 water–ethanol mixture. The chemical analyses of **1** and **2** were in agreement with the structures described hereafter.

Crystallographic data collection and structure determination

All measurements were carried out at room temperature on an Enraf-Nonius CAD4 diffractometer using graphite-monochromated Mo Kα radiation ($\lambda = 0.71073$ Å). Cell parameters were determined from least-squares refinement of 25 centered reflections The crystal data for $CoCu(obp)(H_2O)_3 \cdot H_2O$ (**1**) are summarized in Table 1, and for $NiCu(obp)(H_2O)_5 \cdot 3.5H_2O$ (**2**) in Table 2. The data were corrected for Lorentz and polarization effects, and for absorption by the Gaussian integration method. The scattering curves, with anomalous dispersion terms included, were those of Cromer and Waber [8]. All calculations were carried out on a MICRO-VAXII computer using the Enraf-Nonius structure determination programs [9].

TABLE 1. Crystallographic data for $CoCu(obp)(H_2O)_3 \cdot H_2O$ (1)

Chemical formula	$C_8H_{16}N_2O_{10}CuCo$
Formula weight	422.70
Space group	$P\bar{1}$ (No 2)
a (Å)	8 642(1)
b (Å)	9 197(1)
c (Å)	10.645(2)
α (°)	67 14(1)
β (°)	62.28(1)
γ (°)	73 95(1)
V (Å^3)	685.4(2)
Z	2
T (°C)	21
λ (Å)	0.71073
ρ_{obs} (g cm^{-3})	2.1
ρ_{calc} (g cm^{-3})	2 048
μ (cm^{-1})	28.179
Transmission coefficient	0.477–0.755
$R(F_o)$	0 024
$R_w(F_o)$	0 030

TABLE 2 Crystallographic data for $NiCu(obp)(H_2O)_5 \cdot 3.5H_2O$ (2)

Chemical formula	$C_{16}H_{50}N_4O_{29}Cu_2Ni_2$
Formula weight	1007.09
Space group	$P\bar{1}$
a (Å)	11.444(1)
b (Å)	12.295(1)
c (Å)	15.100(2)
α (°)	68.89(1)
β (°)	72 94(1)
γ (°)	76.26(1)
V (Å^3)	1874 1(3)
Z	2
T (°C)	21
λ (Å)	0.71073
ρ_{obs} (g cm^{-3})	1 8
ρ_{calc} (g cm^{-3})	1.785
μ (cm^{-1})	22.176
Transmission coefficient	0 57–0.83
$R(F_o)$	0.049
$R_w(F_o)$	0 047

$CoCu(obp)(H_2O)_3 \cdot H_2O$ (1)

The intensity distribution clearly favors a centrosymmetric space group, hence $P\bar{1}$ was chosen and proved to be correct in the course of the work. The structure was solved by direct methods. The atomic positions revealed in the E-map were in agreement with those of $MnCu(obp)(H_2O)_3 \cdot H_2O$, confirming that the CoCu and MnCu compounds are isomorphous. Refinement was performed with a full-matrix least-squares method. After anisotropic refinement, hydrogen atoms were located from difference Fourier maps, and were included in the refinement. In the final cycles of refinement an isotropic extinction parameter was also included and adjusted. The refinement based on 2923 reflections with $|F| > 32\sigma$ converged at $R = 0.024$, $R_w = 0.030$, $s = 2.022$. Atomic parameters are listed in Table 3, and bond lengths and angles for non-hydrogen atoms in Tables 4 and 5.

$NiCu(obp)(H_2O)_5 \cdot 3.5H_2O$ (2)

Although the intensity distribution was in accordance with a centrosymmetric space group, attempts of solving the structure in space group $P\bar{1}$ were not successful. The structure was eventually solved by direct methods in the non-centrosymmetric space group $P1$ with four independent molecules per asymmetric unit. During the subsequent refinement it became evident that the molecules were pairwise centrosymmetrically related, and the refinement was successfully completed in the centrosymmetric space group. All non-hydrogen atoms were anisotropically refined. Hydrogen atoms on carbon

TABLE 3. Atomic parameters for non-hydrogen atoms in $CoCu(obp)(H_2O)_3 \cdot H_2O$ (1)

Atom	x	y	z	B_{eq}[a] (Å^2)
Cu	−0.01136(3)	0.23788(3)	0.46710(2)	1.490(5)
Co	0.25478(3)	0.14610(3)	−0.06703(2)	1.494(5)
O1	0.3279(2)	0.2070(2)	0.0653(1)	1.70(3)
O2	0.0208(2)	0.1226(2)	0.1303(1)	1.64(3)
O3	0.0905(2)	0.3069(2)	0.5635(1)	1.85(3)
O4	−0.2124(2)	0.1693(2)	0.6541(1)	1.77(3)
O5	0 2106(2)	0.4867(2)	0.5666(1)	2.69(3)
O6	−0.4908(2)	0.1483(2)	0.7873(2)	3.30(4)
O7	0.3081(2)	−0.1083(2)	0.0198(1)	2.19(3)
O8	0.1800(2)	0 3956(2)	−0.1503(2)	3.41(4)
O9	0.1417(2)	0.1164(2)	−0.1831(1)	2.79(3)
O10	0 2238(2)	0.5962(2)	−0.0214(2)	4.54(6)
N1	0.2026(2)	0.2631(2)	0.2882(2)	1.68(3)
N2	−0.0890(2)	0.1647(2)	0.3591(2)	1.60(3)
C1	0.0299(2)	0.1619(2)	0.2283(2)	1.33(4)
C2	0.2042(2)	0.2147(2)	0.1886(2)	1.34(4)
C3	0 3555(2)	0 3266(2)	0.2619(2)	2.03(4)
C4	0.2965(3)	0.4606(2)	0.3297(2)	2.03(4)
C5	0.1937(2)	0.4154(2)	0.4978(2)	1.66(4)
C6	−0.2621(2)	0.1165(2)	0.4154(2)	1.83(4)
C7	−0.3986(2)	0.1999(2)	0.5284(2)	1.82(4)
C8	−0 3656(2)	0.1700(2)	0.6643(2)	1.64(4)

[a] $B_{eq} = (4/3)\Sigma_i \Sigma_j \beta_{ij} \mathbf{a}_i \cdot \mathbf{a}_j$.

TABLE 4. Bond distances (Å) involving non-hydrogen atoms for $CoCu(obp)(H_2O)_3 \cdot H_2O$ (1)

Cu–O3	1.971(1)	Co–O8	2.145(2)	N1–C3	1.457(2)
Cu–O4	1 948(1)	Co–O9	2.022(1)	N2–C1	1.295(2)
Cu–O5[1]	2.640(1)	O1–C2	1.264(2)	N2–C6	1.456(2)
Cu–N1	1.928(1)	O2–C1	1.269(2)	C1–C2	1.529(2)
Cu–N2	1.948(1)	O3–C5	1 285(2)	C3–C4	1.516(2)
Co–O1	2.082(1)	O4–C8	1.275(2)	C4–C5	1.520(2)
Co–O2	2.118(1)	O5–C5	1.231(2)	C6–C7	1 524(2)
Co–O6[2]	2.017(1)	O6–C8	1.234(2)	C7–C8	1.510(2)
Co–O7	2.159(1)	N1–C2	1.293(2)		

Symmetry operations: [1] $-x, 1-y, 1-z$, [2] $1+x, y, z-1$.

atoms (except on the disordered C7A) and coordinated water molecules (except on O11B) were located in a difference Fourier map, and isotropically refined. The full-matrix least-squares refinement converged to $R = 0.049$, $R_w = 0.047$, $s = 1.00$. Atomic parameters are listed in Table 6, bond lengths and angles for non-hydrogen atoms in Tables 7 and 8.

Magnetic measurements

These were carried out in the 4.2–300 K temperature range with a Faraday-type magnetometer equipped with an Oxford Instruments helium continuous-flow cryostat. $HgCo(NCS)_4$ was used as a susceptibility standard. Diamagnetic corrections were taken as -180×10^{-6} and -230×10^{-6} cm^3 mol^{-1} for **1** and **2**, respectively.

Description of the crystal structures

$CoCu(obp)(H_2O)_3 \cdot H_2O$ (1)

The compound is isostructural with $MnCu(obp)(H_2O)_3 \cdot H_2O$, the structure of which has already been described [1]. The structure consists of bimetallic chains where the Co(II) and Cu(II) ions are bridged alternatingly by oxamido and carboxylato groups, as shown in Fig. 1. The Cu atoms within one chain have long axial bonds to the carboxylato O5 atoms in a centrosymmetrically related chain, forming double chains as shown in Fig. 2. These double chains run parallel to the [10-1] direction. The Co atom has somewhat distorted octahedral surroundings with two oxamido oxygen atoms, one carboxylato oxygen atom and one water molecule in equatorial positions, and two water molecules in axial positions. The Co–O bond lengths are on average 0.07 Å shorter than the Mn–O bond lengths in the isostructural compound. The equatorial ligand atoms deviate significantly from planarity (−0.130, 0.152, −0.142, 0.121 Å for O6[2], O1, O2 and O9, respectively), while the Co atom lies in the plane (see 'Supplementary material', Table SV). The Cu atom is in distorted square-pyramidal surroundings with two oxamido nitrogen atoms (av. Cu–N = 1.938 Å) and two carboxylato oxygen atoms (av. Cu–N = 1.960 Å) in equatorial positions, the apical position being occupied by a carboxylato oxygen atom from a centrosymmetrically related chain (Cu–O = 2.640 Å). There are only minor differences between the Mn and Co isostructural compounds in bond lengths and angles around copper. N1, N2, O3 and O4 deviate by −0.070, 0.069, 0.065 and −0.064 Å, respectively, from the mean equatorial plane, the Cu atom being displaced 0.110 Å from this plane towards the apical position. The dihedral angle between the equatorial planes of Co and Cu is 12.9°.

Within a single chain the Co and Cu atoms are bridged by an oxamido group O1O2C1C2N1N2 with a Co···Cu separation of 5.369 Å on one hand, and by a carboxylato group O4C8O6 with a Co···Cu separation of 5.998 Å on the other hand. The corresponding values in the isostructural MnCu compound are 5.452 and 6.066 Å, respectively, the difference being due to longer Mn–O bond lengths. In both compounds the carboxylato group is in the *anti–anti* configuration, the C8–O6–Co[3] angle (157.0°) being slightly larger than the corresponding angle in the MnCu compound (154.9°). The oxamido bridge makes dihedral angles of 9.3 and 8.6° with the equatorial planes of Co and Cu, respectively, and of 26.4° with the carboxylato bridge. The angles between the plane of the carboxylato bridge and the equatorial planes are 17.9 and 25.2°, respectively. All these dihedral angles are close to those of the MnCu structure. The metal atoms deviate significantly from the planes of both bridges; the deviations from

TABLE 5. Bond angles (°) involving non-hydrogen atoms for $CoCu(obp)(H_2O)_3 \cdot H_2O$ (1)

O3–Cu–O4	91.78(4)	O2–Co–O9	93.50(5)	O2–C1–N2	129 1(1)
O3–Cu–O5^1	90.12(4)	O6^2–Co–O7	88.12(6)	O2–C1–C2	116.6(1)
O3–Cu–N1	91.11(5)	O6^2–Co–O8	95 82(6)	N2–C1–C2	114.3(1)
O3–Cu–N2	174.52(5)	O6^2–Co–O9	101 49(6)	O1–C2–N1	129.0(1)
O4–Cu–O5^1	84 34(4)	O7–Co–O8	175 06(6)	O1–C2–C1	117.1(1)
O4–Cu–N1	169 09(5)	O7–Co–O9	90.19(6)	N1–C2–C1	114.0(1)
O4–Cu–N2	92.86(5)	O8–Co–O9	86 11(7)	N1–C3–C4	109 9(1)
O5^1–Cu–N1	106.18(5)	Co–O1–C2	114.01(9)	C3–C4–C5	115.9(1)
O5^1–Cu–N2	93.24(4)	Co–O2–C1	113 00(9)	O3–C5–O5	122.0(1)
N1–Cu–N2	83.80(5)	Cu–O3–C5	125.31(9)	O3–C5–C4	119.7(1)
O1–Co–O2	79 02(4)	Cu–O4–C8	124 41(9)	O5–C5–C4	118.3(1)
O1–Co–O6^2	87.02(5)	Co^3–O6–C8	157.0(1)	N2–C6–C7	110.6(1)
O1–Co–O7	97.17(5)	Cu–N1–C2	114.28(9)	C6–C7–C8	116.0(1)
O1–Co–O8	86.04(6)	Cu–N1–C3	125.40(9)	O4–C8–O6	119.6(1)
O1–Co–O9	168.96(5)	C2–N1–C3	120.3(1)	O4–C8–C7	121 5(1)
O2–Co–O6^2	163.57(5)	Cu–N2–C1	113.40(9)	O6–C8–C7	118.9(1)
O2–Co–O7	85.11(5)	Cu–N2–C6	125 00(9)	Cu^1–O5–C5	107 1(1)
O2–Co–O8	91.84(5)	C1–N2–C6	121.6(1)		

Symmetry operations: ^{1} $-x, 1-y, 1-z$; ^{2} $1+x, y, z-1$; ^{3} $x-1, y, 1+z$.

the oxamido plane are 0.131 and −0.065 Å for Co and Cu, respectively, and from the carboxylato plane 0.191 and 0.314 Å.

Within the double chain the Cu···Cu' separation is 5.201 Å, slightly longer than in the MnCu derivative, due to a longer Cu–O5 distance and a larger Cu'–O5–C5 angle. The shortest metal···metal separations occur between neighboring double chains, Cu···Cu($-x$, $-y$, $1-z$) being 4.117(1) Å (compared to 4.262 Å in MnCu), and Co···Co($1-x$, $-y$, $-z$) being 4.855 Å (compared to 4.819 Å in MnCu). The double chains are laced together through hydrogen bonding (see 'Supplementary material', Table SIV).

$NiCu(obp)(H_2O)_5 \cdot 3.5H_2O$ (2)

The asymmetric unit consists of two neutral heterodinuclear units, shown in Fig. 3, each of formula $NiCu(obp)(H_2O)_5$, and seven molecules of uncoordinated water. There are only minor differences in bond distances and angles between the two crystallographically independent molecules noted A and B. Each Ni atom has slightly distorted octahedral surroundings, being coordinated to two oxygen atoms of the oxamido group and four water molecules. Each Cu atom is five-coordinated in a square pyramidal geometry with the oxamido nitrogen atoms and two carboxylic oxygen atoms in the equatorial plane, and a water molecule in the axial position. The Cu–O11 axial bond is somewhat longer in molecule A than in molecule B (2.477 versus 2.345 Å), and the tetrahedral distortion of the equatorial ligands are slightly more noticeable in this molecule A (see 'Supplementary material', Table SX). The Cu atoms are displaced by 0.200 Å and 0.219 Å, respectively, from the equatorial plane towards the apical ligand. The Ni atoms deviate by only 0.004 and 0.020 Å from the equatorial planes. The dihedral angles between the Cu and Ni equatorial planes are 12.1(3) and 12.4(3)° for molecules A and B, respectively. The Ni···Cu intramolecular separations are 5.307(1) and 5.320(1) Å.

The surroundings of the two molecules in the crystal lattice are different, as evidenced by the hydrogen-bond pattern and the various intermolecular metal···metal separations. The hydrogen atoms of O2 and O10 are, for example, oriented differently in the two molecules due to the effect of hydrogen bonding. See also 'Supplementary material', Table SIX. The shortest intermolecular metal···metal separations are NiA···NiB(x, $1-y$, z) = 4.885 Å and NiA···NiA($-x$, $1+y$, $1-z$) = 4.961 Å. Other contacts less than 6 Å are: CuB···NiA($-x$, $1-y$, $-z$) = 5.208 Å, CuA···NiB($1-x$, $-y$, $1-z$) = 5.295 Å, CuB···CuB($-x$, $-y$, $-z$) = 5.663 Å, and CuA···CuA($1-x$, $1-y$, $1-z$) = 5.691 Å.

Magnetic properties

$CoCu(obp)(H_2O)_5 \cdot H_2O$ (1)

The magnetic properties of the Co(II)Cu(II) compound are shown in Fig. 4 in the form of the $\chi_M T$ versus T plot, χ_M being the molar magnetic susceptibility and T the temperature. At 290 K, $\chi_M T$ is equal to 2.93 $cm^3\ K\ mol^{-1}$, and decreases more and more rapidly as the temperature is lowered. When T tends to the absolute zero, $\chi_M T$ tends to zero, which indicates that the system has no first-order angular momentum in its ground state. At the first view these results are rather surprising. Indeed, from the crystal structure we could anticipate to observe the one-dimensional ferrimagnetic

TABLE 6. Atomic parameters for non-hydrogen atoms in $NiCu(obp)(H_2O)_5 \cdot 3.5H_2O$ (2)

Atom	x	y	z	B_{eq}[a] (Å^2)
CuA	0.48483(4)	0.29482(4)	0.46063(4)	1.65(1)
CuB	0.16500(5)	0.16801(4)	−0.07745(3)	1.67(1)
NiA	0.10503(4)	0.58114(4)	0.32632(3)	1.29(1)
NiB	0.24963(5)	−0.05358(4)	0.27706(3)	1.41(1)
O1A	0.1372(2)	0.4205(2)	0.4313(2)	1.51(6)
O1B	0.1873(3)	0.1124(2)	0.1954(2)	1.80(6)
O2A	0.2876(2)	0.5790(2)	0.3126(2)	1.64(6)
O2B	0.2450(3)	−0.0930(2)	0.1571(2)	1.69(6)
O3A	0.5104(3)	0.1409(3)	0.5560(2)	2.21(7)
O3B	0.1082(3)	0.3317(2)	−0.1472(2)	2.29(7)
O4A	0.6413(3)	0.3238(3)	0.4731(2)	2.10(7)
O4B	0.1105(3)	0.1160(3)	−0.1674(2)	2.15(6)
O5A	0.4536(3)	−0.0220(3)	0.6653(2)	2.60(7)
O5B	0.0640(3)	0.5227(3)	−0.1713(2)	3.01(8)
O6A	0.7869(3)	0.4265(3)	0.4471(2)	2.87(7)
O6B	0.0772(3)	−0.0200(3)	−0.2166(2)	2.88(7)
O7A	0.0602(2)	0.6697(2)	0.4310(2)	1.59(6)
O7B	0.0684(3)	−0.0846(3)	0.3415(2)	2.03(7)
O8A	0.1423(3)	0.4884(3)	0.2260(2)	2.39(7)
O8B	0.4277(3)	−0.0102(3)	0.2175(2)	2.38(7)
O9B	0.3215(3)	−0.2232(3)	0.3390(2)	2.35(7)
O9A	0.0987(3)	0.7347(3)	0.2143(2)	1.98(6)
O10A	−0.0794(2)	0.5990(2)	0.3373(2)	1.77(6)
O10B	0.2535(3)	−0.0198(3)	0.3998(2)	2.42(7)
O11A	0.5983(3)	0.2371(3)	0.3134(3)	3.34(8)
O11B	0.3661(4)	0.1901(4)	−0.1720(3)	4.6(1)
O12	0.1411(4)	0.7574(3)	−0.2572(3)	3.79(9)
O13	0.5437(4)	0.2575(4)	−0.1122(3)	3.9(1)
O14	0.0759(4)	−0.0954(4)	0.5613(3)	4.9(1)
O15	0.4468(4)	0.2053(4)	0.0867(3)	5.3(1)
O16	0.3609(4)	0.5671(4)	0.0872(3)	5.2(1)
O17	0.5513(5)	0.3726(5)	0.1229(4)	6.1(1)
O18	0.2330(7)	0.2570(4)	0.2842(3)	9.2(2)
N1A	0.3081(3)	0.2938(3)	0.4795(3)	1.73(8)
N1B	0.1711(3)	0.2073(3)	0.0353(2)	2.00(8)
N2B	0.1961(3)	0.0063(3)	0.0078(2)	1.98(8)
N2A	0.4497(3)	0.4525(3)	0.3754(3)	2.14(8)
C1B	0.2123(4)	−0.0010(3)	0.0902(3)	1.61(8)
C1A	0.3363(3)	0.4828(3)	0.3669(3)	1.43(8)
C2A	0.2519(4)	0.3916(3)	0.4312(3)	1.45(8)
C2B	0.1884(4)	0.1165(3)	0.1100(3)	1.62(8)
C3A	0.2416(4)	0.1968(4)	0.5446(3)	2.1(1)
C3B	0.1509(5)	0.3258(4)	0.0415(3)	2.9(1)
C4B	0.1896(5)	0.4127(4)	−0.0579(3)	2.6(1)
C4A	0.3260(4)	0.0804(4)	0.5528(3)	2.12(9)
C5A	0.4350(4)	0.0660(3)	0.5958(3)	1.78(9)
C5B	0.1149(4)	0.4243(4)	−0.1292(3)	1.91(9)
C6A	0.5420(5)	0.5297(5)	0.3221(5)	4.9(1)
C6B	0.2067(5)	−0.1001(4)	−0.0187(3)	2.8(1)
C7B	0.2332(5)	−0.0730(4)	−0.1271(3)	2.8(1)
C8A	0.6944(4)	0.4133(4)	0.4272(3)	2.10(9)
C8B	0.1321(4)	0.0118(4)	−0.1724(3)	1.97(9)
C7A1	0.6667(7)	0.4821(8)	0.3274(6)	2.0(2)
C7A2	0.6262(8)	0.5327(7)	0.3674(7)	2.2(2)

[a] $B_{eq} = (4/3)\Sigma_i \Sigma_j \beta_{ij} \mathbf{a}_i \mathbf{a}_j$.

behavior with a characteristic minimum in the $\chi_M T$ versus T plot, and a rapid increase of $\chi_M T$ upon cooling below the temperature of this minimum [10]. Such a

TABLE 7 Bond distances (Å) involving non-hydrogen atoms for $NiCu(obp)(H_2O)_5 \cdot 3.5H_2O$ (2)

CuA–O3A	1.940(3)	CuB–O3B	1.958(3)
CuA–O4A	1.979(3)	CuB–O4B	1.989(4)
CuA–O11A	2.477(4)	CuB–O11B	2.345(4)
CuA–N1A	1.961(4)	CuB–N1B	1.952(4)
CuA–N2A	1.927(3)	CuB–N2B	1.955(3)
NiA–O1A	2.072(2)	NiB–O1B	2.051(2)
NiA–O2A	2.033(3)	NiB–O2B	2.055(3)
NiA–O7A	2.108(3)	NiB–O7B	2.078(3)
NiA–O8A	2.100(4)	NiB–O8B	2.084(3)
NiA–O9A	2.035(3)	NiB–O9B	2.033(3)
NiA–O10A	2.033(3)	NiB–O10B	2.054(4)
O1A–C2A	1.275(5)	O1B–C2B	1.268(5)
O2A–C1A	1.279(4)	O2B–C1B	1.280(4)
O3A–C5A	1.275(5)	O3B–C5B	1.285(6)
O4A–C8A	1.257(5)	O4B–C8B	1.272(6)
O5A–C5A	1.234(4)	O5B–C5B	1.239(5)
O6A–C8A	1.241(6)	O6B–C8B	1.242(7)
N1A–C2A	1.291(5)	N1B–C2B	1.295(4)
N1A–C3A	1.454(5)	N1B–C3B	1.453(6)
N2A–C1A	1.294(5)	N2B–C1B	1.281(6)
N2A–C6A	1.446(6)	N2B–C6B	1.469(7)
C1A–C2A	1.521(5)	C1B–C2B	1.525(6)
C3A–C4A	1.511(6)	C3B–C4B	1.507(5)
C4A–C5A	1.516(7)	C4B–C5B	1.511(8)
C6A–C7A1	1.423(9)	C6B–C7B	1.498(7)
C6A–C7A2	1.35(1)	C7B–C8B	1.508(6)
C8A–C7A1	1.52(1)		
C8A–C7A2	1.580(8)		

TABLE 8. Bond angles (°) involving non-hydrogen atoms for $NiCu(obp)(H_2O)_5 \cdot 3.5H_2O$ (2)

O3A–CuA–O4A	87.5(1)	O3B–CuB–O4B	89.1(1)
O3A–CuA–O11A	97.2(1)	O3B–CuB–O11B	89.5(1)
O3A–CuA–N1A	94.2(1)	O3B–CuB–N1B	93.0(1)
O3A–CuA–N2A	174.9(1)	O3B–CuB–N2B	170.6(1)
O4A–CuA–O11A	89.6(1)	O4B–CuB–O11B	96.4(2)
O4A–CuA–N1A	161.3(2)	O4B–CuB–N1B	163.0(1)
O4A–CuA–N2A	93.2(1)	O4B–CuB–N2B	92.4(2)
O11A–CuA–N1A	108.6(2)	O11B–CuB–N1B	100.5(2)
O11A–CuA–N2A	87.9(1)	O11B–CuB–N2B	99.5(1)
N1A–CuA–N2A	83.5(1)	N1B–CuB–N2B	82.9(2)
O1A–NiA–O2A	81.9(1)	O1B–NiB–O2B	81.5(1)
O1A–NiA–O7A	90.9(1)	O1B–NiB–O7B	90.1(1)
O1A–NiA–O8A	87.8(1)	O1B–NiB–O8B	87.4(1)
O1A–NiA–O9A	172.1(1)	O1B–NiB–O9B	171.5(1)
O1A–NiA–O10A	102.3(1)	O1B–NiB–O10B	100.2(1)
O2A–NiA–O7A	89.8(1)	O2B–NiB–O7B	90.8(1)
O2A–NiA–O8A	92.5(1)	O2B–NiB–O8B	93.2(1)
O2A–NiA–O9A	91.0(1)	O2B–Nib–O9B	90.7(1)
O2A–NiA–O10A	174.9(1)	O2B–NiB–O10B	178.1(1)
O7A–NiA–O8A	177.2(1)	O7B–NiB–O8B	174.9(1)
O7A–NiA–O9A	92.6(1)	O7B–NiB–O9B	93.3(1)
O7A–NiA–O10A	87.3(1)	O7B–NiB–O10B	88.4(1)
O8A–NiA–O9A	89.0(1)	O8B–NiB–O9B	89.8(1)
O8A–NiA–O10A	90.5(1)	O8B–NiB–O10B	87.8(1)
O9A–NiA–O10A	85.0(1)	O9B–NiB–O10B	87.7(1)

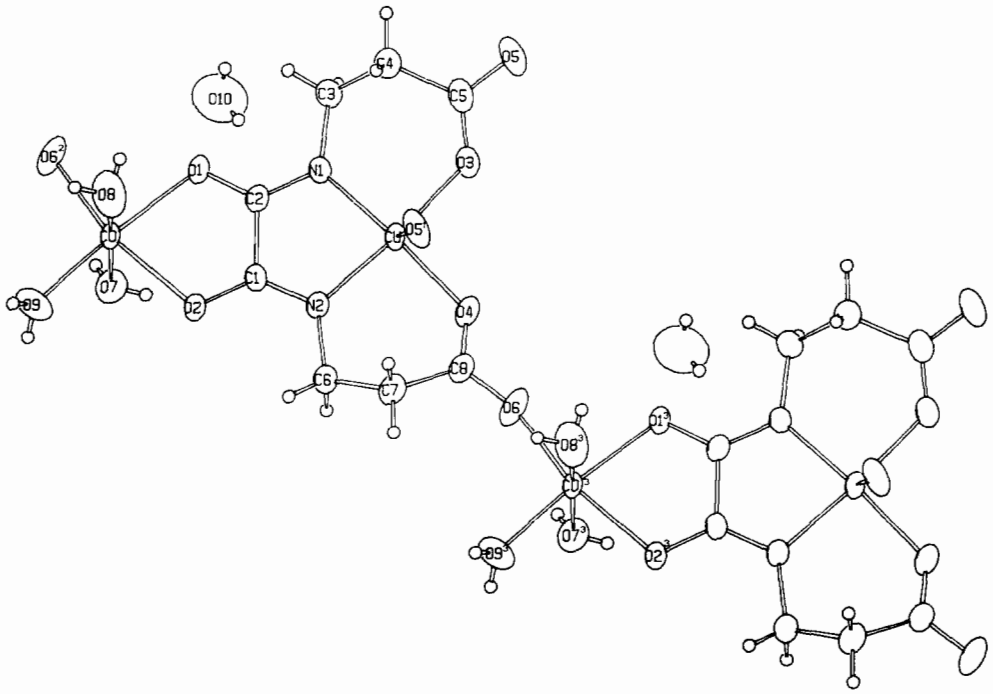

Fig. 1 Section of single chain in $CoCu(obp)(H_2O)_3\ H_2O$ (**1**) showing the atomic numbering used Thermal ellipsoids for non-hydrogen atoms are plotted at the 70% probability level. Hydrogen atoms are given an arbitrary radius

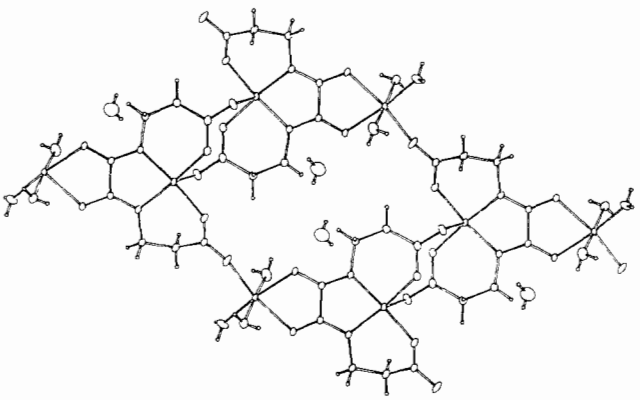

Fig. 2. Section of a double chain in $CoCu(obp)(H_2O)_3 \cdot H_2O$ (**1**).

behavior was observed for the bimetallic chain compound $CoCu(pbaOH)(H_2O)_3 \cdot 2H_2O$ which exhibits a minimum in the $\chi_M T$ versus T plot at 53 K [11]. The situation for $CoCu(obp)(H_2O)_3 \cdot H_2O$ is obviously more complicated since there is now alternation not only of the spin carriers, Co(II) and Cu(II), but of the interaction pathways as well, oxamido and carboxylato. In $MnCu(obp)(H_2O)_3 \cdot H_2O$ the interaction parameter through the carboxylato bridge ($J_2 = -6.8$ cm^{-1}) was found to be much weaker than that through the oxamido bridge ($J_1 = -32.0$ cm^{-1}), and in some other Mn(II)Cu(II) alternating bimetallic chains involving both oxamido and carboxylato bridges the interaction through the latter bridge was found to be negligibly small. This happens when the coordination around the carboxylato bridge is of the *syn–anti* type [3, 4, 7]. In the case of $CoCu(obp)(H_2O)_3 \cdot H_2O$ the absence of minimum in the $\chi_M T$ versus T curve does not necessarily imply that the J(carboxylato) interaction parameter through the carboxylato bridge is negligibly small. Let us make clear this apparent paradox. The ratio J(carboxylato)/J(oxamido) is certainly very small, if not zero. Therefore, we may describe the system as consisting of chains of oxamido-bridged Co(II)Cu(II) units denoted P, ferromagnetically coupled through the carboxylato bridge. This coupling between P units in a certain sense may be viewed as a weak perturbation with regard to the dominant intra-unit interaction [6].

Let us neglect in a first time this perturbation, and consider the magnetic behavior of isolated P units. The quantitative interpretation of the magnetic properties for a Co(II)Cu(II) dinuclear entity in which the Co(II) ion is in a weak octahedral field is far from being trivial [10]. The difficulties arise from the presence of a first-order orbital momentum for a Co(II) ion in a $^4T_1$ state. The rhombic distortion with respect to the ideal octahedral symmetry undergone by the Co(II) ion splits the $^4T_2$ state into three spin-quartet orbital-singlet states, each of them being further split into two Kramers doublets by the spin–orbit coupling. At low temperature only the ground Kramers doublet of Co(II) is thermally populated, carrying an effective spin $S'_{Co} = 1/2$, and the

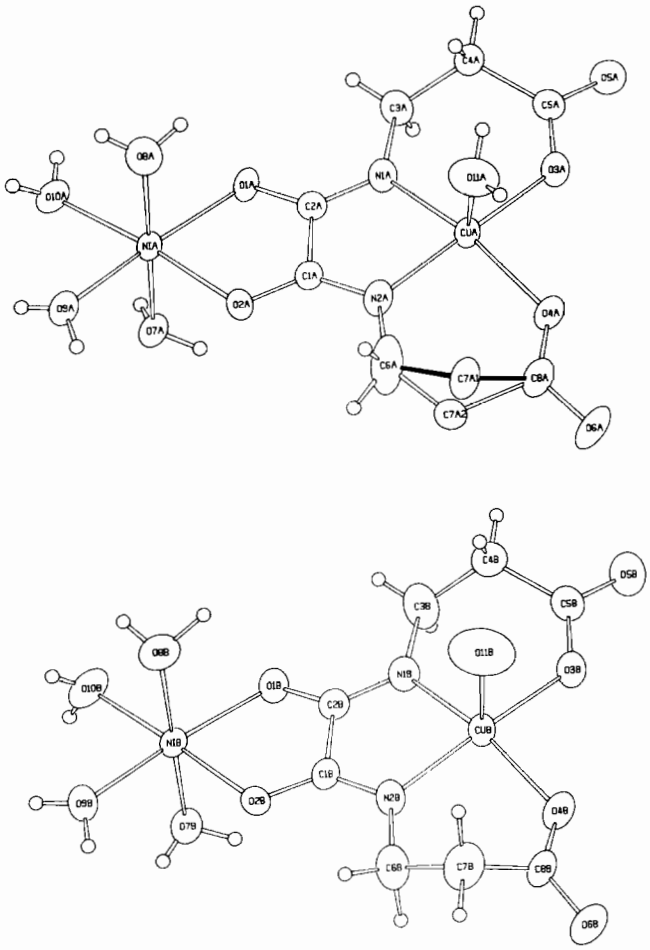

Fig. 3 The two molecules of $NiCu(obp)(H_2O)_5$ in the asymmetric unit of $NiCu(obp)(H_2O)_5$ (**2**). Thermal ellipsoids are shown at the 70% probability level.

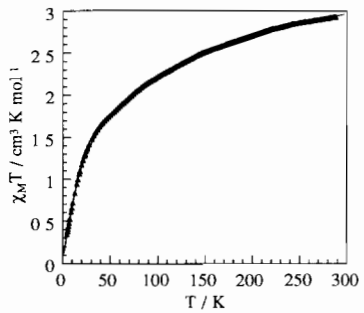

Fig. 4 $\chi_M T$ vs. T plot for $CoCu(obp)(H_2O)_3 \cdot H_2O$ (**1**). ▲, experimental points; —, calculated curve.

interaction with the $S_{Cu} = 1/2$ Kramers doublet of Cu(II) may actually give rise to a non-magnetic ground state.

We now introduce the weak coupling between P units. Since the ground state of P is non-magnetic, this coupling, provided that it is weak enough, gives rise to a chain with again a non-magnetic ground state, and $\chi_M T$ is expected to tend to zero as T approaches the absolute zero, even if J(carboxylato) is not zero. It follows that J(carboxylato) may be very difficult, if not impossible, to deduce from the magnetic data, and we decided to see whether a pair model could properly reproduce the $\chi_M T$ versus T curve.

Some years ago one of us proposed a phenomenological model to describe the Co(II)Cu(II) interaction, taking into account the orbital degeneracy of the Co(II) ion in octahedral environment. We do not think that it is necessary to recall here all the details on this model. The readers who are interested are referred to refs. 10 and 12. We limit ourselves to the reminder that the zero-field Hamiltonian takes the form:

$$\mathcal{H} = \mathcal{H}_{Co} + \mathcal{H}_{Cu} + \mathcal{H}_{CoCu} \quad (1)$$

$\mathcal{H}_{Co}$ explicitly takes into account the local distortion and the spin–orbit coupling for the Co(II) ion; in other words the eigenstates of $\mathcal{H}_{Co}$ are six Kramers doublets. The eigenstate of $\mathcal{H}_{Cu}$ is the ground Kramers doublet for Cu(II). As for $\mathcal{H}_{CoCu}$, it is defined as:

$$\mathcal{H}_{CoCu} = -\mathbf{J}\mathbf{S}_{Co} \cdot \mathbf{S}_{Cu} \quad (2)$$

where **J** is not a scalar but an orbital operator acting on the pair functions obtained as products of the local functions and transforming as the irreducible representations Γ of the group describing the symmetry properties of the Co(II)Cu(II) entity (close to C_{2v}), according to:

$$\langle \Gamma | \mathbf{J} | \Gamma' \rangle = J_{\Gamma\Gamma} \delta_{\Gamma\Gamma'} \quad (3)$$

In the present case there are in principle three J_Γ interaction parameters. The Zeeman perturbation is finally expressed as the sum of the local contributions:

$$\mathcal{H}_{ZE} = \mathcal{H}_{ZE,Co} + \mathcal{H}_{ZE,Cu} \quad (4)$$

with

$$\mathcal{H}_{ZE,Co} = \beta H (k_{Co} \mathbf{L}_{Co} + g_{Co} \mathbf{S}_{Co}) \quad (5)$$

$$\mathcal{H}_{ZE,Cu} = \beta H g_{Cu} \mathbf{S}_{Cu} \quad (6)$$

where $\mathcal{H}$ is the applied magnetic field, $\mathbf{L}_{Co}$ the orbital momentum operator for Co(II), k_{Co} the orbital reduction factor, the other symbols having their usual meaning. The apparent defect of this model might be its overparametrization, but owing to the intrinsic complexity of the problem, perhaps it is not possible to describe the magnetic properties of a Co(II)Cu(II) pair in a more simple way. In the present case we imposed the values of the spin–orbit coupling parameter within the ^4F free-ion ground state of Co(II) ($\lambda = 160$ cm^{-1}), and of the orbital reduction factor ($k_{Co} = 0.9$). Furthermore we supposed that the local distortion around Co(II) was axial with a D energy gap between the ground orbital singlet and the excited orbital doublet, and that the three interaction parameters J_Γ were equal, and looked for an 'effective' J value. This last approximation

is certainly the most severe, and the least justified theoretically. In this frame quite a good fitting of the experimental curve was obtained for $J = -60$ cm^{-1}, $D = 800$ cm^{-1}, $g_{Co} = g_{Cu} = 2.08$. The agreement factor defined as $\Sigma[(\chi_M T)^{obs} - (\chi_M T)^{calc}]^2/[(\chi_M T)^{obs}]^2$ is then equal to 5.3×10^{-5} (for 165 experimental points). The quality of the fitting stopped us from looking for an alternative model taking into account the interaction through the carboxylato bridge. It probably makes more sense to say that, owing to the complexity of the model, J(carboxylato) is weak enough to prevent the ferrimagnetic behavior, but remains undetermined.

NiCu(obp)(H$_2$O)$_5$·3.5H$_2$O (2)

The $\chi_M T$ versus T plot is shown in Fig. 5. At room temperature $\chi_M T$ is equal to 1.33 cm^3 K mol^{-1}, decreases as the temperature is lowered, and finally reaches a plateau below *c.* 40 K with $\chi_M T = 0.45$ cm^3 K mol^{-1}. This behavior is quite typical of an isolated Ni(II)Cu(II) heteropair with antiferromagnetic intramolecular interaction. The plateau below 40 K corresponds to the temperature range where only the ground doublet state is thermally populated. These magnetic data allow a rather accurate determination of the doublet–quartet energy gap $3J/2$, where **J** is the interaction parameter occurring in the spin Hamiltonian $-\mathbf{J}\mathbf{S}_{Ni} \cdot \mathbf{S}_{Cu}$. The theoretical expression for $\chi_M T$ is [10, 13]:

$$\chi_M T = (N\beta^2/4kT)[g_{1/2}^2 + 10g_{3/2}^2 \exp(3J/2kT)]/ [1 + 2\exp(3J/2kT)] \quad (7)$$

where the symbols have their usual meaning. The least-squares fitting of the data leads to $3J/2 = -150.7$ cm^{-1} with $g_{1/2} = 2.32$ and $g_{3/2} = 2.16$. The agreement factor defined as above is then equal to 2.7×10^{-5} (for 152 experimental points). The $g_{1/2}$ and $g_{3/2}$ factors are related to the local g_{Ni} and g_{Cu} factors through [14, 15]:

$$g_{1/2} = (4g_{Ni} - g_{Cu})/3$$
$$g_{3/2} = (2g_{Ni} + g_{Cu})/3 \quad (8)$$

which leads to $g_{Ni} = 2.24$ and $g_{Cu} = 2.0$.

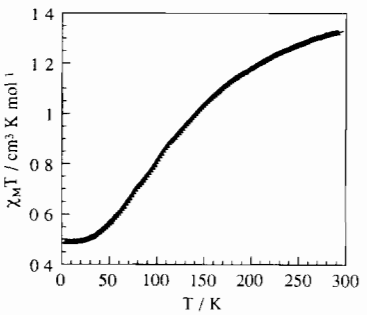

Fig. 5. $\chi_M T$ vs T plot for NiCu(obp)(H$_2$O)$_5$·3.5H$_2$O (**2**): ▲, experimental points; —, calculated curve

Conclusions

This work emphasizes once more the remarkable versatility of bimetallic compounds incorporating ligands of the oxamido(*N*,*N'*-carboxylato) type as to their structures and magnetic properties. Using obp = oxamidobis(*N*,*N'*-propionato), we synthesized the Co(II)Cu(II) and Ni(II)Cu(II) species. The structure of the former compound consists of alternating bimetallic chains. This structure had already been encountered for MnCu(obp)(H$_2$O)$_3$·H$_2$O. The magnetic behavior of this Co(II)Cu(II) species, on the other hand, does not show the expected ferrimagnetic regime. The magnetic data may be interpreted with a model of a Co(II)Cu(II) pair in which the orbital degeneracy of the Co(II) ion in a weak octahedral field is fully taken into account. The structure of the Ni(II)Cu(II) compound consists of isolated heterodinuclear units, and the magnetic behavior is fully in line with such a structure. The interaction between the Ni(II) and Cu(II) ions gives rise to doublet and quartet pair states, with a doublet–quartet energy gap of $3J/2 = -150.7$ cm^{-1}. The magnitude of this antiferromagnetic interaction confirms the capability of the oxamido bridge to transmit the electronic effects between magnetic centers rather far away from each other [10].

At this stage it seemed to us worthwhile to compare the interaction parameters through the oxamido bridge in MCu(obp) type species with M = Mn, Co and Ni. These parameters have been found as $J_{MnCu} = -32$ cm^{-1}, $J_{CoCu} = -60$ cm^{-1} and $J_{NiCu} = -100.5$ cm^{-1}. These J_{MCu} parameters are related to contributions involving pairs of magnetic orbital through [10]:

$$J_{MCu} = (1/S_M S_{Cu})\Sigma_\mu J_{\mu b1} \quad (9)$$

where the index μ in $J_{\mu b1}$ stands for the symmetry of the magnetic orbital centered on M, and the index b_1 for the symmetry of the unique magnetic orbital centered on Cu. S_M and S_{Cu} (= 1/2) in (9) are the local spins. For the three compounds the dominant contribution accounting for the strong antiferromagnetic interaction is J_{b1b1} involving magnetic orbitals located in the plane of the bridging network. Neglecting the other contributions and assuming that J_{b1b1} is constant whatever M should result in the relation:

$$5J_{MnCu} \approx 3J_{CoCu} \approx 2J_{NiCu} \quad (10)$$

The J_{MCu} values deduced from the experimental magnetic data are not too far from the values suggested by this relation (10). However, the equal signs have to be replaced by the signs <, which may be attributed to the fact that the number of ferromagnetic contributions $J_{\mu b1}$ with $\mu \neq b_1$ increases along the series NiCu < CoCu < MnCu.

The FeCu(obp) and Cu_2(obp) species have not yet been obtained. For these two compounds the J_{b1b1} contribution is again expected to be dominant, and from what precedes, it is possible to predict the order of magnitude of the interaction parameters as $J_{FeCu} \approx -43$ cm^{-1} and $J_{CuCu} \approx -200$ cm^{-1}. It is also possible to predict that the interaction in the hypothetical CrCu(obp) compound should be ferromagnetic ($J_{CrCu} > 0$). Indeed, owing to the Jahn-Teller distortion of the Cr(II) ion, the b_1 orbital centered on this ion is empty, and the J_{b1b1} contribution vanishes. The beauty of molecular magnetism to a large extent is due to this harmony between versatility and unexpected findings on the one hand, and possibility to predict the nature and the order of magnitude of the phenomena on the other hand.

Supplementary material

Details of the crystallographic data, anisotropic thermal parameters for non-hydrogen atoms, bond distances and angles involving hydrogen atoms, hydrogen bonds, least-squares planes and dihedral angles (Tables SI–SX), and listings of structure factors for **1** and **2** are available on request from author O.K.

References

1 Y Pei, O Kahn, J Sletten, J.P. Renard, R. Georges, J.C. Gianduzzo, J Curely and Q. Xu, *Inorg. Chem*, *27* (1988) 41
2 K. Nakatani, J.Y. Carriat, Y Journaux, O. Kahn, F. Lloret, J P. Renard, Y. Pei, J. Sletten and M. Verdaguer, *J Am Chem Soc*, *111* (1989) 5739.
3 Y. Pei, K. Nakatani, O. Kahn, J. Sletten and J.P. Renard, *Inorg Chem.*, *28* (1989) 3170.
4 K Nakatani, J Sletten, S. Halut-Desporte, S. Jeannin, Y. Jeannin and O. Kahn, *Inorg Chem*, *30* (1991) 164.
5 Y. Pei. O. Kahn, K. Nakatani, E Codjovi, C. Mathonière and J Sletten, *J Am. Chem. Soc.*, *113* (1991) 6558
6 F. Lloret, M Julve, R. Ruiz, Y. Journaux, K. Nakatani, O. Kahn and J. Sletten, *Inorg Chem*, *32* (1993) 27.
7 O. Kahn, Y. Pei, K. Nakatani, Y. Journaux and J. Sletten, *New J Chem*, *16* (1992) 269
8 D.T. Cromer and J.T. Waber, *International Tables for X-Ray Crystallography*, Vol. IV, Kynoch, Birmingham, UK, 1974, p. 99, Table 2.2B.
9 B.A. Frez, *The SDP-User's Guide (SDPVAX V.3)*, Enraf-Nonius, Delft, Netherlands, 1985.
10 O. Kahn, *Molecular Magnetism*, Verlag Chemie, New York, 1993.
11 P.J. van Koningsbruggen, O. Kahn, K. Nakatani, Y Pei, J.P. Renard, M. Drillon and P. Legoll, *Inorg. Chem*, *29* (1990) 3325.
12 O Kahn, P. Tola and H. Coudanne, *Chem. Phys*, *42* (1979) 355.
13 O Kahn, *Struct. Bonding(Berlin)*, *68* (1987) 89.
14 R.P. Scaringe, D. Hodgson and W E. Hatfield, *Mol Phys*, *35* (1978) 701.
15 D. Gatteschi and A. Bencini, in R.W. Willett, D. Gatteschi and O. Kahn (eds.), *Magneto-Structural Correlations in Exchange Coupled Systems*, NATO ASI Series, Dordrecht, Netherlands, 1985.